STRENGTH PREDICTION OF BOLTED JOINTS IN CROSS-PLY LAMINATES BASED ON SUBCRITICAL DAMAGE MODELLING

A. Ataş[1,2*], A. Hodzic[1‡], C. Soutis[1†]

[1]*Department of Mechanical Engineering, The University of Sheffield, Sheffield S1 3JD, U.K*
[2]*Department of Mechanical Engineering, Balikesir University, Balikesir 10145, Turkey*
*a.atas@sheffield.ac.uk, ‡a.hodzic@sheffield.ac.uk, †c.soutis@sheffield.ac.uk

Keywords: Composite bolted joints, strength prediction, subcritical damage modelling, cohesive zone elements (CZEs).

Abstract
A strength prediction method based on subcritical damage modelling is presented for double-lap single fastener bolted joints in cross-ply carbon fibre reinforced plastic (CFRP) laminates loaded in tension. Three-dimensional (3-D) finite element (FE) models were developed and cohesive zone elements (CZEs) were inserted into subcritical damage planes identified from X-ray radiographs. Strength of the joints was determined from the predicted load-displacement curves; scaling effects at sub-laminate and ply-level were also considered. The proposed method provides a universally applicable strength prediction tool for the bolted joints in composite laminates without referring to empirical correlation factors.

1 Introduction

The extensive use of carbon fibre reinforced plastic (CFRP) composite materials has been mainly driven by the stringent competitive conditions of aircraft industry (reduced weight, fuel and noise) which has increased steadily over the past decades. The primary reasons of the high demand for the CFRP composites are their outstanding specific stiffness and strength properties which in turn lead to substantial weight reductions. These advantages, however, may not be fully utilised unless designing the structural joints efficiently.

The joint efficiency of ductile metals is shown to be as high as twice of the CFRP composites due to their high stress concentration relief around the fastener hole boundaries based on extensive yielding capability [1]. Thus, the design of structural joints in composite laminates is of great importance in order to compete with those ductile metal structures. CFRP laminates also show some stress concentration relief although each of its constituents (the resin matrix and fibres) behaves in a brittle manner up to failure. Subcritical damage modes such as transverse matrix cracks, fibre pull-outs, axial splits and delaminations between adjacent layers contribute to that stress concentration relief [2] and provided that they don't grow under fatigue loading conditions they could be considered as beneficial.

Most of the strength prediction techniques to date (characteristic curve, stress concentration reduction factor, progressive failure analysis) rely on some form of empirical correlation

factors in order to take the subcritical damage modes into account [2-4]. These correlation factors are functions of the material system, joint geometry, clamping torque, laminate lay-up and stacking sequence. This empirical dependency of the strength prediction methods obviously limits their application for general use.

The aim of this paper is to present a strength prediction method for bolted joints in CFRP laminates based on subcritical damage modelling which relies little on measured data and is relatively independent of correction or correlation factors. The locations of the subcritical damage modes were determined first using the X-ray radiography technique. CZEs were than inserted into those locations to simulate the onset and growth of the subcritical damage modes, as detailed in the subsequent sections.

2 Materials and testing methods

The material system used in this study is HTS40/977-2 carbon fibre-epoxy in the form of pre-impregnated (prepreg) tape. The prepreg tapes were made of unidirectional high tensile strength/standard modulus aerospace grade carbon fibres (Toho Tenax®, HTS40-F13-12K-800tex) pre-impregnated with 177˚C curing toughened epoxy resin (Cycom®977-2). The nominal thickness of the prepreg tape is 0.25mm with an approximate fibre volume fraction of 58% [5]. The composite laminates were fabricated by the hand lay-up technique in an autoclave according to the manufacturer's recommended curing procedure. Typical specimen geometry is shown in Fig. 1 with definitions of the width (w), free edge distance (e), hole diameter (d) and thickness (t). The x-y and 1-2 coordinate systems define the global laminate and local material coordinate systems, respectively and the angle θ defines the layer orientation angle with respect to the x (loading) axis and also the circumferential co-ordinate direction around the hole boundary.

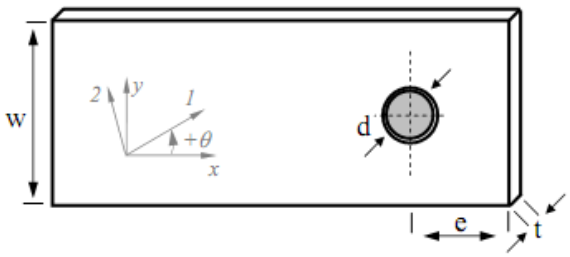

Figure 1. Geometrical definitions of a bolt-loaded composite laminate.

A diamond tip saw was used to cut the laminates to dimensions with special care given to the precise alignment of the laminates. Fastener holes were drilled with a backing plate in order to prevent drilling induced delamination failure. The laminates were inspected by X-ray radiography to establish specimen quality. Double-lap single-bolted shear loading fixtures were manufactured in accordance with the ASTM standard D5961/D5961 [6]. 12.9 grade steel bolts of 5.95mm in diameter were used to load the specimens. Tests were conducted at room temperature with a Hounsfield electromechanical testing machine, at a 1 mm/min loading rate. Applied load and the cross-head displacement were recorded by a computer aided data acquisition system. Tests were stopped after a significant (approximately 30 %) load drop was observed in the load-displacement curve, according to ASTM standard [6]. Finger-tightened joints were chosen according to standard design practices where the fully-

tightened joints are assumed to be loosened due to service loading conditions. After testing, specimens were inspected using penetrant enhanced X-ray radiography [7].

Cross-ply specimens are often not used in practical structural applications. They were used in this work, however, as benchmarks due to their relatively apparent damage locations to facilitate comparison with the FE predictions and test theoretical damage models and assumptions. Three cross-ply lay-ups, as shown in Table 1, were tested considering the effect of sublaminate-level ($[90^\circ/0^\circ]_{2s}$) and ply-level ($[90_2^\circ/0_2^\circ]_s$) scaled laminates on the strength of bolted joints [8]. Laminates with 90˚ outer layers were used to provide the same degree of constraint for the inner 0˚ layers [9]. The width-to-hole diameter and edge distance-to-hole diameter ratios were kept constant (w/d=6 and e/d=3).

Laminate lay-up	Specimen code	w/d	e/d
$[90^\circ/0^\circ]_s$	B1W	6	3
$[90^\circ_2/0^\circ_2]_s$	B2W	6	3
$[90^\circ/0^\circ]_{2s}$	B3W	6	3

Table 1. Cross-ply bolted joint specimen test parameters.

3 Experimental observations

An X-ray radiograph of a finger-tight bolted joint in the $[90^\circ/0^\circ]_s$ lay-up (B1W) is shown in Fig. 2, where transverse matrix cracks, axial splitting, compressive fibre failure and delamination damage can be observed.

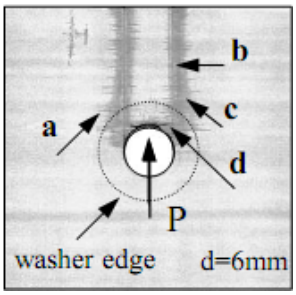

B1W (w/d=6, e/d=3)

Figure 2. An X-ray radiograph showing damage in a finger-tight bolted $[90^\circ/0^\circ]_s$ lay-up at failure: a) transverse matrix cracks, b) axial splitting, c) delamination, d) compressive fibre failure in 0˚ layers.

Figure 3 shows a schematic of the subcritical in-plane damage locations observed from the X-ray radiographs of the cross-ply lay-ups.

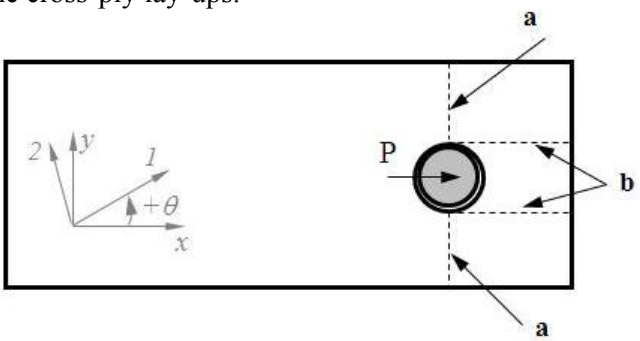

Figure 3. Subcritical in-plane damage locations observed in cross-ply lay-ups: a) transverse matrix cracking planes in 90˚ layers, b) axial split planes in 0˚ layers.

The extent of the transverse matrix cracks dispersed along the axial splits as shown in X-ray radiographs. However, it has been shown that those transverse matrix cracks can be represented as a single crack where the maximum stress concentration occurs for the centre notched specimens [10]. Thus, based on this assumption, the transverse matrix cracks were represented as single cracks at the maximum stress concentration locations ($\theta = \pm 90^{\circ}$). Axial split planes within the 0° layers were extended from the hole edge at $\theta = \pm 90^{\circ}$ to the free edge as observed from the radiographs and depicted schematically in Fig.3.

4 Finite element modelling

Finite element models (3-D) were developed using the ANSYS software [11] based on the subcritical damage planes shown in Fig. 3 and delamination planes between the adjacent layers. Elastic material properties, strengths and interfacial properties of the HTS40/977-2 are given in Tables 2 to 4. The interfacial properties were adopted from T300/977-2 CFRP material system owing to the same toughened epoxy matrix material used for both pre-pregs. Together with the high strength fibres of similar characteristics (HTS40 and T300), both material systems also exhibit very close elastic material properties [12]. The interfacial properties, Table 4, were used to model both the axial splits (within the 0° layers) and delamination subcritical damage modes through the CZEs [11].

E_{11} (MPa)	$E_{22}=E_{33}$ (MPa)	$G_{12}=G_{13}$ (MPa)	G_{23} (MPa)	$\nu_{12}=\nu_{13}$	ν_{23}
153000	10300	5200	3430	0.3	0.5

Table 2. Elastic properties of HTS40/977-2 [13].

X_T (MPa)	X_C (MPa)	$Y_T = Z_T$ (MPa)	$Y_C = Z_C$ (MPa)	$S_{XY} = S_{XZ} = S_{YZ}$ (MPa)
2540	1500	82	236	90

Table 3. Strengths of HTS40/977-2 [13].

G_{IC} (N/mm)	G_{IIC} (N/mm)	σ_{max} (MPa)	τ_{max} (MPa)	K_n (N/mm^3)	K_t (N/mm^3)
0.352	1.45	60	80	$1x10^5$	$1x10^5$

Table 4. Interfacial properties used for HTS40/977-2 adopted from T300/977-2 [12, 14].

Before attempting to predict the strength of bolted joints , it is necessary to verify the FE model predictions using experimental measurements, such as split length as a function of applied stress. However, damage in pin/bolt loaded laminates initiates at 90-95% of the ultimate load, which makes it quite difficult to measure the split/delamination growth as a function of the applied load. A previous experimental study [15] showed that, in a cross-ply $[90^{\circ}/0^{\circ}]_s$ centre notched laminate under tensile loading, axial splitting within the 0° layers was initiated at the notch tips at relatively lower loads. They grew progressively along the fibre direction accompanied by delamination between adjacent layers. Owing to that progressive subcritical damage evolution, a cross-ply $[90^{\circ}/0^{\circ}]_s$ laminate with a centre notch was modelled to validate the current FE modelling approach [16, 17]. A good correlation was obtained between the subcritical damage predictions of the current nonlinear FE model and the experimental results [15]. Together with the correlation of the contact stress distributions [17], this confirms that the subcritical damage onset and growth of the bolted joints in CFRP laminates can be predicted with a reasonably good accuracy.

4 Results and discussions

Figure 4 shows the experimental and predicted load-displacement curves of the B1W specimen as an example. The load increases in a nonlinear fashion due to the initiation of the subcritical damage modes at early stages of loading up to point A, where the maximum load of the joint is reached. After that point, the load decreases with increased displacement since the resistance of the remaining undamaged part of the specimen ahead of the fastener reduces with increased length of the subcritical damage.

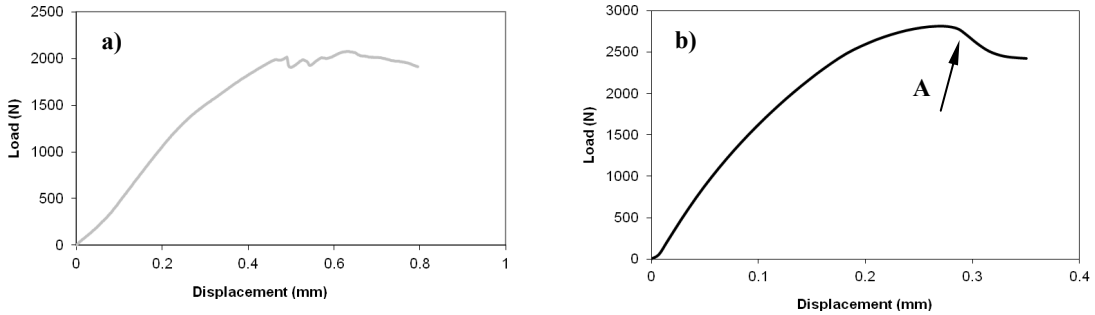

Figure 4. a) Experimental and b) predicted load-displacement curve of $[90^{\circ}/0^{\circ}]_s$ specimen (B1W).

The bearing strength of the bolted joint specimens was determined by using Eq. 1, based on the maximum load carried by the joint (P_{max}) which was obtained from the numerical load-displacement curve such as that shown in Fig. 4b.

$$S_{max} = P_{max} / dt \tag{1}$$

where d and t are the hole diameter and specimen thickness, respectively. Figures 5 and 6 show the predicted delamination damage at the 90˚/0˚ interface and the splitting damage within the 0˚ layers of the B1W specimen at the maximum load, around point A, in Fig. 4.

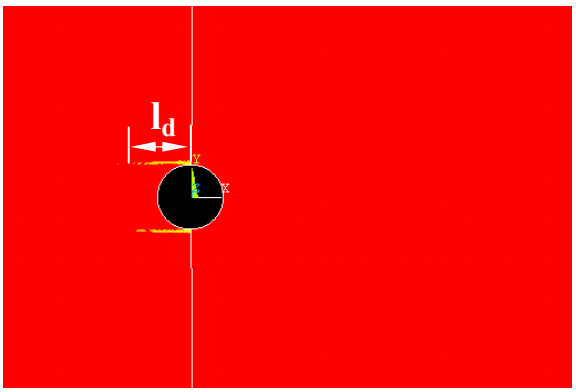

Figure 5. Delamination damage at the 90˚/0˚ interface of $[90^{\circ}/0^{\circ}]_s$ specimen at maximum load (l_d: delamination length=6 mm).

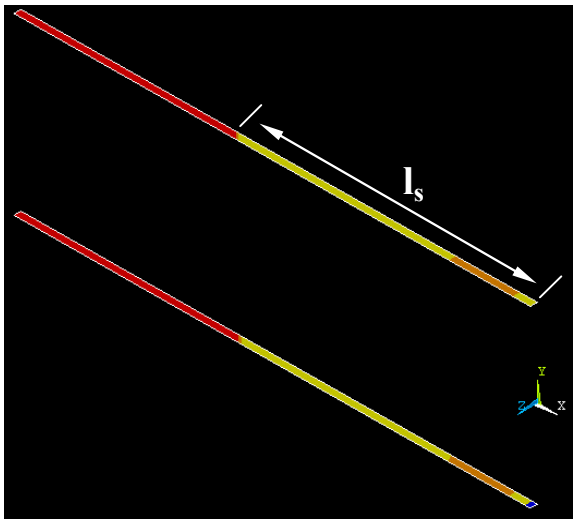

Figure 6. Splitting damage within the 0˚ layers of $[90˚/0˚]_s$ specimen at maximum load associated with the delamination damage in Fig. 5 (l_s: split length=10 mm).

The approximate length of the delamination (l_d) and the splitting damages (l_s) are 6mm and 10mm, respectively, which agrees with the suggestion that the splitting drives the delamination damage [9, 10].

Experimental bearing strength of the joints was determined from the load-displacement curves after a significant load drop was observed according to ASTM standard [6], as stated earlier. Therefore, the X-ray radiographs of the failed specimens do not correspond to the maximum load carried by the joints in which the splits and other subcritical damage modes were extended up to the free edges of the specimens. This is the reason of relatively short lengths of the delamination and splits in Figs. 5 and 6, which were captured at the maximum load, but not the ultimate failure load. In order to show the ability of the modelling approach, Fig. 7 was captured when the delamination was reached at the free edge with increased bolt displacement. The agreement of the prediction with the X-ray radiograph, Fig. 2, is very good.

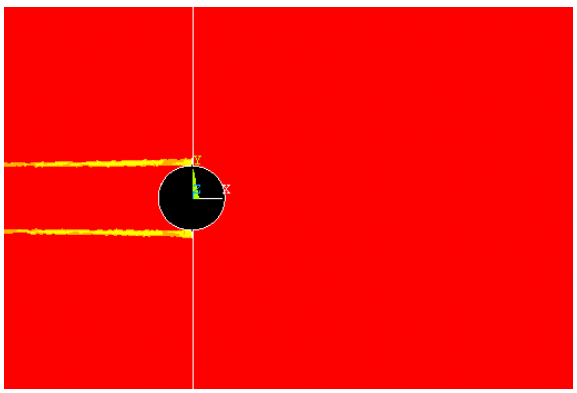

Figure 7. Delamination damage at the 90˚/0˚ interface of $[90˚/0˚]_s$ specimen with increased displacement after the maximum load.

Figure 8 compares the predicted and experimental (average of minimum five specimens) bearing strengths of the cross-ply specimens. The maximum difference is approximately 20%

for the B1W specimen and the agreement is much improved for B2W and B3W specimens. The increased strength of the sublaminate-level scaled B3W specimen was attributed to the interspersion of the layers, explained as follows. The global mode of failure observed in the experiments was shear-out [17] in which the splitting within the 0˚ layers and the delaminations between the consecutive layers join up and shear-out the laminate ahead of the fastener (generally, as wide as the fastener diameter). Blocking the layers together (ply-level scaling), instead of interspersion, has a twofold effect on the strength of those joints. First, the splits initiate at the hole edge and grow through-the-thickness of the blocked layers without an interruption from the adjacent layers. Second, ply-level scaling reduces the number of interfaces and therefore increases the magnitude of the shear stress to be carried by each interface [18]. As a result, greater delamination was developed under lower load levels for the ply-level scaled $[90^{\circ}_2/0^{\circ}_2]_s$ lay-up (B2W) with a broader extent of transverse matrix cracking. Although this could result in stronger joints in a quasi- or near quasi-isotropic lay-up that fails in net-tension mode, by providing better stress concentration relief [19], the larger delamination size caused global shear-out mode failure for the B2W cross-ply lay-up. Hence, the blocked-ply laminate configuration should be avoided due to poorer shear properties.

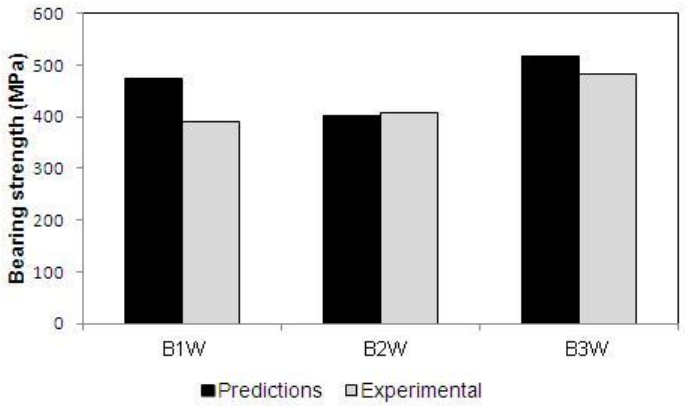

Figure 8. Predicted and experimental bearing strengths for the cross-ply lay-ups (e/d=3, w/d=6).

5 Conclusions

The success of currently used strength prediction methods for bolted joints is strongly dependant on several laminate, geometry and material system related parameters. This dependency stems from the variations in the extent of the subcritical damage modes and is generally compensated with various forms of correlation factors. The motivation of the present study was to develop a strength prediction method, based on subcritical damage modelling, which is universally applicable without resorting to experimentally determined correlation factors. Therefore, 3-D FE models were developed and the CZEs were embedded into those subcritical damage locations determined from the X-ray radiographs. CZEs use a strength-based failure criterion to predict the damage onset and a fracture mechanics based approach to predict its growth. Thus, the material properties required for simulating the subcritical damage modes were only the interfacial strength and fracture energies of the particular material system used. The strength of the joints was accurately determined from the predicted load-displacement curves. It has been shown that the effect of various laminate stacking sequences (scaling effect) on the joint strength was accounted for by the method developed.

Acknowledgements

The authors acknowledge the Balikesir University and Turkish Council of Higher Education (YÖK) for the PhD scholarship awarded to Mr A. Ataş.

References

[1] Hart-Smith LJ. Design and analysis of bolted and riveted joints in fibrous composite structures. In: L.Tong, C.Soutis, editors. Recent Advances in Structural Joints and Repairs for Composite Materials: Kluwer Academic Publishers; 2003. p. 211-54.
[2] Hart-Smith LJ. Bolted Joints in Graphite-epoxy composites. Douglas Aircraft Company, NASA Langley Report NASA CR-144899; 1976.
[3] Camanho PP, Matthews FL. A progressive damage model for mechanically fastened joints in composite laminates. Journal of Composite Materials. 1999;33:2248-80.
[4] Chang FK, Scott RA, Springer GS. Strength of Mechanically Fastened Composite Joints. Journal of Composite Materials. 1982;16:470-94.
[5] Jumahat A, Soutis C, Jones FR, Hodzic A. Fracture mechanisms and failure analysis of carbon fibre/toughened epoxy composites subjected to compressive loading. Composite Structures. 2010;92:295-305.
[6] ASTM. D 5961/D 5961M – 01 Standard Test Method for Bearing Response of Polymer Matrix Composite Laminates. United States2001.
[7] Soutis C, Fleck NA, Curtis PT. Hole Hole Interaction in Carbon-Fiber Epoxy Laminates under Uniaxial Compression. Composites. 1991;22:31-8.
[8] Soutis C, Lee J. Scaling effects in notched carbon fibre/epoxy composites loaded in compression. Journal of Materials Science. 2008;43:6593-8.
[9] Kortschot MT, Beaumont PWR. Damage Mechanics of Composite-Materials .1. Measurements of Damage and Strength. Composites Science and Technology. 1990;39:289-301.
[10] Wisnom MR, Chang FK. Modelling of splitting and delamination in notched cross-ply laminates. Composites Science and Technology. 2000;60:2849-56.
[11] ANSYS® Academic Research, Release 12.1. 2009.
[12] Goyal VK, Johnson ER, Davila CG. Irreversible constitutive law for modeling the delamination process using interfacial surface discontinuities. Composite Structures. 2004;65:289-305.
[13] Heimbs S, Heller S, Middendorf P, Hahnel F, Weisse J. Low velocity impact on CFRP plates with compressive preload: Test and modelling. International Journal of Impact Engineering. 2009;36:1182-93.
[14] Harper PW, Hallett SR. Cohesive zone length in numerical simulations of composite delamination. Engineering Fracture Mechanics. 2008;75:4774-92.
[15] Spearing SM, Beaumont PWR. Fatigue Damage Mechanics of Composite-Materials .1. Experimental-Measurement of Damage and Post-Fatigue Properties. Composites Science and Technology. 1992;44:159-68.
[16] Atas A, Mohamed GF, Soutis C. Effect of clamping force on the delamination onset and growth in bolted composite laminates. Composite Structures. 2012;94:548-52.
[17] Atas A, Mohamed G, Soutis C. Modelling delamination onset and growth in pin loaded composite laminates. Composites Science and Technology. 2011:DOI:10.1016/j.compscitech.2011.07.005.
[18] Mandell JF, Wang SS, Mcgarry FJ. Extension of Crack Tip Damage Zones in Fiber Reinforced Plastic Laminates. Journal of Composite Materials. 1975;9:266-87.
[19] Hart-Smith LJ. Mechanically-Fastened Joints for Advanced Composites - Phenomenological Considerations and Simple Analyses. In: Lenoe EM, Oplinger DW, J.J.Burke, editors. Fibrous Composites in Structural Design: Plenum Press, New York; 1980. p. 543-74.